Applied Magnetic Resonance (2023) 54:905–913
https://doi.org/10.1007/s00723-023-01559-2

Applied
Magnetic Resonance

ORIGINAL PAPER

Ionic Mobility in Metallic Sodium Nanoparticles Confined to Porous Glass

A. V. Uskov[1] · D. Yu. Nefedov[1] · E. V. Charnaya[1] · V. M. Mikushev[1] · M. K. Lee[2] · L.-J. Chang[2] · Yu. A. Kumzerov[3] · A. V. Fokin[3]

Received: 27 May 2023 / Revised: 24 June 2023 / Accepted: 26 June 2023 /
Published online: 1 July 2023

Abstract

Metallic sodium nanoparticles can be used in numerous applications. This requires thorough investigation of their properties. To study the impact of size reduction on the ionic mobility in solid sodium, we carried out ^{23}Na NMR measurements of the Knight shift and spin–lattice relaxation for sodium nanoparticles embedded into a porous glass with a mean pore size of 23 nm and in bulk sodium. Pronounced acceleration of relaxation in nanoparticles compared to bulk was revealed within a temperature range from 190 to 293 K, while the Knight shift nearly coincided with that in bulk solid sodium. In addition, the rate of magnetization recovery after inversion depended on magnetic field and the recovery curves were non-single exponential. The results were treated assuming the emergence of a noticeable quadrupole contribution to relaxation due to coupling of nuclear quadrupole moments with electric field gradients caused by ionic mobility intensified under nanoconfinement. The correlation time of ionic mobility was found for sodium nanoparticles at different temperatures. The activation energy was evaluated and was shown to be much smaller than in bulk solid sodium.

1 Introduction

Sodium is one of the most abundant element in our environment. Metallic sodium has many applications in chemistry, physics, and medicine, while it is strongly reactive. Modern representative uses of metallic sodium are coolants for nuclear reactors and a potential anode material for rechargeable sodium-based batteries [1]. Recently,

✉ E. V. Charnaya
e.charnaya@spbu.ru

[1] St.-Petersburg State University, St.-Petersburg 198504, Russia

[2] National Cheng Kung University, Tainan 70101, Taiwan

[3] Ioffe Institute RAS, St.-Petersburg 194021, Russia

great attention was paid to studies of metallic sodium nanoparticles because of their feasible practical applications and frequent occurrence in nature. Sodium nanoparticles were introduced for enhanced oil recovery procedure [2–4]. They are considered for production of nanoscale plasmonic devices as small particles of many other metals [5, 6]. The metal Na nanoinclusions cause the bright colors in villiaumite and halite minerals [7]. To remove serious irreversibility problems in metallic sodium anodes, they were suggested to be replaced with three-dimensional nanotemplates loaded with Na [8, 9]. Nanoscale clusters of sodium within pores of silica gel were shown to be convenient materials for chemical reduction of organic compounds and production of clean hydrogen [10]. Sodium nanoparticles are also widespread in the food industry.

Size reduction in sodium nanoparticles affects their physical and structural properties. Previous studies revealed remarkable decreases in the melting and freezing temperatures of small sodium particles [11–13] in agreement with results obtained for other fusible metals (see [14, 15] and references therein). The partial polymorph phase transition, which occurs in bulk sodium below 40 K, was found to shift to 240 K for small sodium particles embedded into a porous glass [16]. NMR measurements demonstrated noticeable changes in the Knight shift for solid and liquid sodium nanoparticles confined to porous glass with a mean pore size of 3.5 nm, which evidenced alterations in the hyperfine coupling [11]. However, nothing is known up to now about the impact of nanostructuring on ionic mobility in solid metallic sodium.

It was shown in [17] that NMR can provide information on self-diffusion in metallic nanoparticles under nanoconfinement through measurements of nuclear spin relaxation. The method is based on separation of the quadrupole contribution to longitudinal relaxation, which depends on the correlation time of ionic mobility. The experiments carried out for liquid gallium and indium and their alloys demonstrated striking slowdown of ionic mobility, which heightened with decreasing the particle sizes [15, 17–20]. Strong NMR line broadening prevented similar studies for solid nanoparticles. The only results were obtained for solid gallium nanosegregates with the β-Ga structure under opal nanoconfinement [21]. The cubic symmetry of metallic sodium facilitates the observation of NMR signals in crystalline sodium nanoparticles allowing the use of NMR to study size-effects on ionic mobility. Here, we present results of NMR measurements of ^{23}Na spin–lattice relaxation within a large temperature range from 190 K to room temperature for sodium nanoparticles embedded into a porous glass with a mean pore size of 23 nm. The temperature dependence of the correlation time of ionic mobility was found and the activation energy was calculated. The enhancement of ionic mobility in solid sodium induced by nanoconfinement was demonstrated.

2 Samples and Experiment

The porous glass template was made from phase-separated sodium-boron-silicate glass by acid leaching. The leaching procedure resulted in formation of thoroughly interconnected network of pores. The pore volume was equal to 18%. The pore size

and distribution were found by nitrogen adsorption–desorption with Quadrasorb SI. The pore size distribution diagram is shown in the inset in Fig. 1. According to this diagram, the mean pore diameter was equal to 23 nm and 80% pores had sizes within a range from 18 to 27 nm.

Metallic sodium was embedded into pores of the glass template in melted state at 400 K under pressure up to 10 kbar. Then, the pressure was removed and the loaded glass was cooled down to room temperature. The pore filling was near 90% as was found by weighing the glass ingot before and after loading. The sample for studies was cut as a parallelepiped with dimensions $3\times3\times5$ mm and sealed into an evacuated ampoule to prevent sodium oxidation. During experiments, the sample was wrapped in a Teflon tape impregnated with oil.

The main NMR measurements were performed using Bruker Avance400 and Avance750 pulse spectrometers in magnetic fields 9.4 and 17.6 T, respectively, within the temperature range from 190 to 293 K upon cooling and warming. The ^{23}Na NMR lines were recorded as a Fourier transform of the free induction decay after a 90° pulse. The line shift was referenced to the ^{23}Na signal from a NaCl single crystal at room temperature. The same reference was used in experiments with bulk sodium [22, 23]. The evolution of spin–lattice relaxation with temperature was studied using the inversion recovery protocol. The temperature changed no faster than 0.5 K/min to avoid temperature overshoots. Before measurements, the sample was kept for 20 min at each target temperature. The Knight shift was also measured within a larger range from 17 up to 415 K using Bruker Avance500 spectrometer to get data on melting reduction under nanoconfinement and on low-temperature behavior of the hyperfine coupling. In addition, the time of nuclear spin–lattice relaxation and Knight shift were measured for bulk metallic sodium. For this, small pieces of sodium were sealed in a silica glass tube.

3 Results and Discussion

The ^{23}Na spectrum at room temperature monitored using the Avance400 spectrometer is shown in Fig. 1. The line at 1123 ± 2 ppm belongs to metallic sodium nanoparticles. Its position is very close to the Knight shift in bulk sodium reported in [22, 23] and to the NMR line shift obtained for bulk sodium in the present study (Fig. 2). The second line at -2.5 ± 1.2 ppm appears due to Na^+ ions [10, 24].

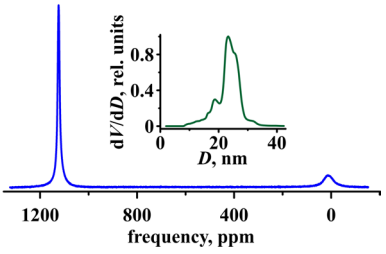

Fig. 1 ^{23}Na NMR spectrum at 293 K obtained with the Avance400 spectrometer. The inset shows the pore diameter distribution diagram

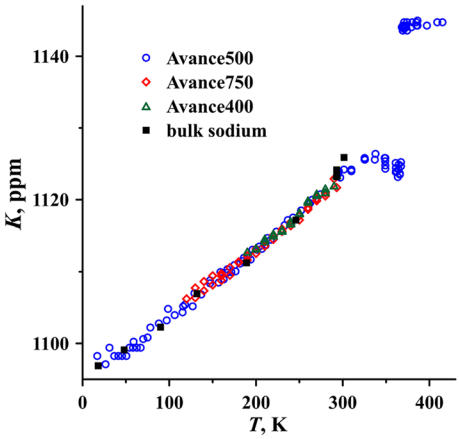

Fig. 2 Temperature dependences of the Knight shift for sodium nanoparticles confined to the glass template measured with three NMR spectrometers and for bulk sodium measured with the Avance400 spectrometer

The temperature dependence of the Knight shift for confined metallic sodium is shown in Fig. 2. We can see that the shifts obtained in different external magnetic fields coincided within experimental data dispersion. The shift jump near 367 K indicates the melting transition, which temperature was slightly dropped compared to bulk sodium because of size-effects [11–13]. Therefore, metallic sodium is solid below room temperature where spin relaxation was studied. Figure 2 demonstrates also that the Knight shift for metallic sodium confined to the glass template with a mean pore size of 23 nm gradually decreases below 293 K with decreasing temperature similar to the Knight shift in bulk in agreement with the results of [23], while the opposite trend was observed for sodium embedded into 3.5 nm pores [11, 16].

Measurements of nuclear magnetization recovery after a 180° pulse revealed pronounced difference between relaxation rates obtained with the Avance400 and Avance750 spectrometers between 190 and 293 K. Examples for 190 and 293 K are shown in Fig. 3. Relaxation was faster at the lower magnetic field. The rate of

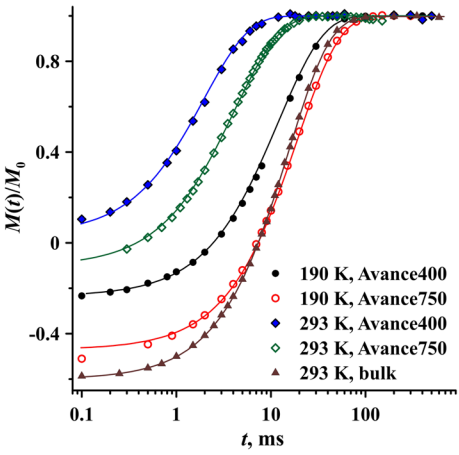

Fig. 3 Nuclear magnetization recovery curves measured for confined sodium nanoparticles using the Avance400 and Avance750 spectrometers at 190 and 293 K and for bulk sodium using the Avance400 spectrometer at 293 K

magnetization recovery increased with increasing temperature. The dependence of the relaxation rate on magnetic field evidences that the extreme narrowing limit is not valid. Moreover, the recovery curves could not be well fitted by single exponentials, while they were close to these functions.

This result is in contrast to spin relaxation measurements for bulk crystalline sodium performed in the present study (Fig. 4) and in [23], which showed that the magnetization recovery was single exponential and the relaxation rate increased linearly with increasing temperature. It was also found in [23] that spin–lattice relaxation did not depend on magnetic field within the range from 70 K to the melting point. Linear variation of the inverse relaxation time with temperature and its independence of magnetic field agree with relaxation due to hyperfine coupling of nuclear magnetic moments with conduction electrons, which dominates in solid and liquid bulk metals [25]. Since the correlation time of electron mobility is short, relaxation via conduction electrons satisfies the extreme narrowing condition.

For nuclei with spin > 1/2, another contribution to spin relaxation in bulk liquid metals was revealed, which realized due to coupling of nuclear quadrupole moments with dynamic gradients of electric fields induced by thermal mobility of ions [26]. This contribution is noticeable only for nuclei with large quadrupole moments such as indium and gallium. The appropriate theoretical relationships were presented in Ref. [27]. Detailed studies reviewed in Ref. [26] showed that coupling of the nuclear magnetic moments with conduction electrons and of the nuclear quadrupole moments with dynamic electric field gradients provides two most effective mechanisms of spin relaxation in liquid metals and metallic alloys.

The quadrupole contribution to relaxation increases remarkably for liquid metallic confined nanoparticles [15, 17–20]. This was proved unambiguously in NMR experiments for two gallium isotopes with different quadrupole moments and gyromagnetic ratios [17]. The quadrupole relaxation acceleration under nanoconfinement was caused by remarkable slowdown of ion mobility, which resulted in the pronounced rise of spectral densities of the electric field gradients' correlation function at the Larmor frequency. In contrast, magnetic relaxation due to coupling

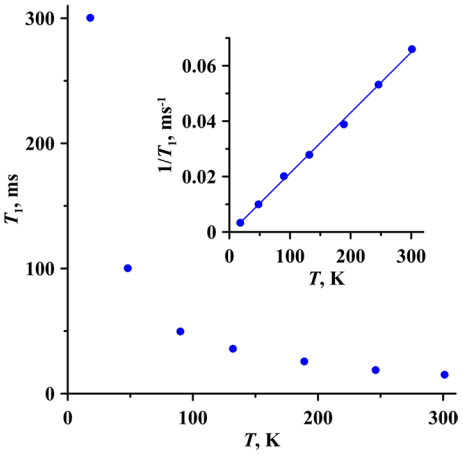

Fig. 4 Temperature dependence of the ^{23}Na spin–lattice relaxation time T_1 obtained for bulk sodium using the Avance400 spectrometer. The inset shows the temperature dependence of the inverse relaxation time

with conduction electrons remains nearly unaffected in agreement with relatively weak impact of nanoconfinement on the Knight shift. The enhancement of quadrupole relaxation ensures acceleration of total spin relaxation in metallic melts under nanoconfinement.

Quadrupole spin–lattice relaxation was not reported for bulk solid metals likely because of slow ionic mobility, which led to small spectral densities of the electric field gradients' correlation function at the Larmor frequency. The only study of spin–lattice relaxation in solid gallium nanoparticles with β-Ga structure embedded into an opal matrix [21] demonstrated a noticeable contribution of quadrupole coupling.

Spin–lattice relaxation in nanoconfined solid sodium is also faster than in bulk as can be seen from an example shown in Fig. 3. Together with the non-single exponential magnetization recovery and dependence of the relaxation rate on magnetic field, this evidences the pronounced contribution of quadrupole relaxation. In this case, the nuclear magnetization recovery with time t is described by [17, 27]

$$\frac{M(t)}{M_0} = 1 - b\left[\frac{4}{5}\exp\left(-\frac{C\tau_c t}{1+4\omega_0^2\tau_c^2}\right) + \frac{1}{5}\exp\left(-\frac{C\tau_c t}{1+\omega_0^2\tau_c^2}\right)\right]\exp\left(-\frac{t}{T_{1m}}\right), \tag{1}$$

where $M(t)$ and M_0 are time-dependent and equilibrium magnetizations, respectively, C is a coefficient proportional to the nuclear quadrupole moment squared and equal to $C = 2\pi^2 C_q^2(1+\eta^2/3)/5$ [21, 27], C_q is the quadrupole constant, η is the asymmetry, τ_c is the correlation time of ionic mobility, ω_0 is the Larmor frequency, and T_{1m} is the time of magnetic relaxation.

Taking into account that spin–lattice relaxation in bulk solid sodium runs due to coupling with conduction electrons and the Knight shift for confined sodium practically coincides with that in bulk metal (Fig. 3), we can assume that the time of magnetic relaxation for sodium nanoparticles is the same as in bulk. Using the data shown in Fig. 4, we can fit simultaneously the recovery curves obtained with two spectrometers and find the fitting parameters τ_c and C. Note that these parameters are evaluated separately when $\omega_0\tau_c \sim 1$. This requirement was shown to be satisfied for temperatures above 240 K. At lower temperatures, the slow mobility approximation is valid and we can find only the C/τ_c ratio. Since the parameter C depends weakly on temperature, we calculated the correlation time τ_c below 240 K assuming C to be independent of temperature and equal to the value found at higher temperatures $C = 1.26 \cdot 10^{12}$ s^{-2}. The Arrhenius plot for the correlation time τ_c is shown in Fig. 5. It proves the thermal activation origin of the ionic mobility and allows calculating the activation energy $E_0 = (0.114 \pm 0.007)$ eV.

The evaluated activation energy can be compared with the results obtained from experimental and theoretical studies of self-diffusion for bulk metallic sodium in [23, 28–30]. The experiments as well as the computer simulations gave for the activation energy below room temperature an estimate of about 0.38 eV, which is much higher than the value obtained in the present study for confined solid sodium nanoparticles. The smaller activation energy corresponds to the acceleration of ionic mobility under nanoconfinement, namely, to the decrease in the τ_c correlation time.

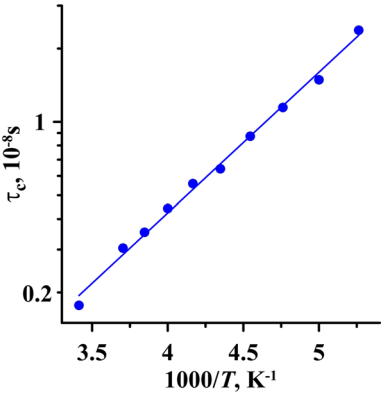

Fig. 5 Dependence of the correlation time of ionic mobility obtained by fitting the experimental recovery curves using Eq. (1) on the inverse temperature. The straight line is the exponential fit corresponding to the Arrhenius plot

This leads to larger spectral densities of the correlation function of electric field gradients at the Larmor frequency and to faster quadrupole relaxation. Up to now, there are no theoretical models, which treat the enhancement of ion migration in small solid metallic particles. However, we can suggest that this effect is related to the greater surface-to-volume ratio and to weakening the inter-ionic potential.

4 Conclusions

^{23}Na NMR studies carried out for solid sodium nanoparticles confined to a porous glass with pore size 23 nm revealed pronounced acceleration of spin–lattice relaxation compared to bulk sodium within a temperature range from 190 to 293 K, while the Knight shift nearly coincided with that in bulk. Since spin relaxation in bulk metallic sodium is known to be caused by coupling of nuclear magnetic moments with conduction electrons, we can assume based on the Korringa relation that the magnetic contribution to relaxation in nanoparticles should be the same as in bulk. Then, the increase in the relaxation rate was ascribed to the emergence of the noticeable quadrupole contribution induced by the rise of ionic mobility. Fitting the nuclear magnetization recovery curves obtained with Avance400 and Avance750 spectrometers gave the correlation time of ionic mobility in sodium nanoparticles at different temperature. This allowed us to evaluate the activation energy, which was much lower than the activation energy found in self-diffusion studies for bulk solid sodium in agreement with faster mobility under nanoconfinement.

Acknowledgements Measurements were carried out using the equipment of the Research Park of St. Petersburg State University.

Author contributions Conceptualization: AVU, EVC, and MKL; methodology: AVU, DYN, VMM, and EVC; formal analysis and investigation: AVU, DYN, and ACF; writing—original draft preparation: AVU and LJC; writing—review and editing: EVC; funding acquisition: YAK; resources: VMM and AVF; supervision: EVC and YAK. All authors read and approved the final manuscript.

Funding The studies were financially supported by the Russian Science Foundation, under Grant no. 21-72-20038.

Availability of data and materials The data sets generated during and/or analyzed during the current study are available from the corresponding author on reasonable request.

Declarations

Conflict of interest The authors have no competing interests.

Ethical approval All procedures performed in studies involving human participants were in accordance with the ethical standards of the institutional and/or national research committee and with the 1964 Helsinki declaration and its later amendments or comparable ethical standards.

Informed consent Informed consent was obtained from all individual participants included in the study.

Consent for publication Consent for publication was obtained for every individual person's data included in the study.

References

1. N. Zhu, M. Xiaoge, G. Wang, M. Zhu, H. Wang, G. Xu, M. Wu, H.K. Liu, S.X. Dou, C. Wu, J. Mater. Chem. A **9**, 13200 (2021). https://doi.org/10.1039/D1TA01800K
2. D. Luo, Z. Ren, Mater. Today Phys. **16**, 100276 (2021). https://doi.org/10.1016/j.mtphys.2020.100276
3. V.E. Katnov, S.A. Trubitsina, A.A. Kayumov, F.A. Aliev, N.A. Nazimov, A.V. Dengaev, A.V. Vakhin, Catal **13**, 609 (2023). https://doi.org/10.3390/catal13030609
4. D. Zareei, D. Luo, K. Kostarelos, Z. Ren, Soft Sci. **1**, 8 (2021). https://doi.org/10.20517/ss.2021.08
5. H. Xiang, X. Zhang, D. Neuhauser, G. Lu, J. Phys. Chem. Lett. **5**, 1163 (2014). https://doi.org/10.1021/jz500216t
6. J.H. Li, M. Hayashi, G.Y. Guo, Phys. Rev. B **88**, 155437 (2013). https://doi.org/10.1103/PhysRevB.88.155437
7. G. Calas, L. Galoisy, A. Geisler, Am. Min. **106**, 838 (2021). https://doi.org/10.2138/am-2021-7917
8. H.J. Yoon, N.R. Kim, H.J. Jin, Y.S. Yun, Adv. Energy Mater. **8**, 1701261 (2018). https://doi.org/10.1002/aenm.201701261
9. W. Luo, Y. Zhang, S. Xu, J. Dai, E. Hitz, Y. Li, C. Yang, C. Chen, B. Liu, L. Hu, Nano Lett. **17**, 3792 (2017). https://doi.org/10.1021/acs.nanolett.7b01138
10. M. Shatnawi, G. Paglia, J.L. Dye, K.C. Cram, M. Lefenfeld, S.J.L. Billinge, J. Am. Chem. Soc. **129**, 1386 (2007). https://doi.org/10.1021/ja067140e
11. A.V. Uskov, D.Y. Nefedov, E.V. Charnaya, E.V. Shevchenko, J. Haase, D. Michel, Y.A. Kumzerov, A.V. Fokin, A.S. Bugaev, Phys. Solid State **58**, 1234 (2016). https://doi.org/10.1134/s1063783416060330
12. C. Hock, M. Schmidt, B. Issendorff, Phys. Rev. B **84**, 113401 (2011). https://doi.org/10.1103/PhysRevB.84.113401
13. E.V. Charnaya, M.K. Lee, L.J. Chang, Y.A. Kumzerov, A.V. Fokin, M.I. Samoylovich, A.S. Bugaev, Phys. Lett. A **379**, 705 (2015). https://doi.org/10.1016/j.physleta.2014.12.028
14. A.A. Vasilev, D.Y. Podorozhkin, D.Y. Nefedov, E.V. Charnaya, V.M. Mikushev, Y.A. Kumzerov, A.V. Fokin, Appl. Magn. Reson. **53**, 1649 (2022). https://doi.org/10.1007/s00723-022-01490-y
15. D.Y. Nefedov, D.Y. Podorozhkin, E.V. Charnaya, A.V. Uskov, J. Haase, Y.A. Kumzerov, A.V. Fokin, J. Phys. Condens. Matter **31**, 255101 (2019). https://doi.org/10.1088/1361-648X/ab1111
16. A.V. Uskov, D.Y. Nefedov, E.V. Charnaya, J. Haase, D. Michel, Y.A. Kumzerov, A.V. Fokin, A.S. Bugaev, Nano Lett. **16**, 791 (2016). https://doi.org/10.1021/acs.nanolett.5b04841
17. E.V. Charnaya, T. Loeser, D. Michel, C. Tien, D. Yaskov, Y.A. Kumzerov, Phys. Rev. Lett. **88**, 097602 (2002). https://doi.org/10.1103/PhysRevLett.88.097602
18. E.V. Charnaya, C. Tien, Y.A. Kumzerov, A.V. Fokin, Phys. Rev. B **70**, 052201 (2004). https://doi.org/10.1103/PhysRevB.70.052201
19. E.V. Charnaya, C. Tien, W. Wang, M.K. Lee, D. Michel, D. Yaskov, S.Y. Sun, Y.A. Kumzerov, Phys. Rev. B **72**, 035406 (2005). https://doi.org/10.1103/PhysRevB.72.035406

20. E.V. Charnaya, M.K. Lee, Y.A. Kumzerov, J. Phys. Condens. Matter **22**, 195108 (2010). https://doi.org/10.1088/0953-8984/22/19/195108
21. D.Y. Nefedov, E.V. Charnaya, A.V. Uskov, A.O. Antonenko, D.Y. Podorozhkin, Y.A. Kumzerov, A.V. Fokin, Phys. Solid State **63**, 1739 (2021). https://doi.org/10.1134/S1063783421100279
22. R. Bertani, M. Mali, J. Roos, D.J. Brinkmann, J. Phys. Condens. Matter **2**, 7911 (1990). https://doi.org/10.1088/0953-8984/2/39/006
23. G. Brünger, O. Kanert, D. Wolf, Phys. Rev. B **22**, 4247 (1980). https://doi.org/10.1103/PhysRevB.22.4247
24. J.L. Dye, P. Nandi, J.E. Jackson, M. Lefenfeld, P.A. Bentley, B.M. Dunyak, F.E. Kwarcinski, C.M. Spencer, T.N. Lindman, P. Lambert, P.K. Jacobson, M.Y. Redko, Chem. Mater. **23**, 2388 (2011). https://doi.org/10.1021/cm2001623
25. J. Winter, *Magnetic Resonance in Metals* (Oxford University Press, Oxford, 1970)
26. J.M. Titman, Phys. Rep. **33**, 1 (1977). https://doi.org/10.1016/0370-1573(77)90060-6
27. P.S. Hubbard, J. Chem. Phys. **53**, 985 (1977). https://doi.org/10.1063/1.1674167
28. E. Smargiassi, Phys. Rev. B **65**, 012301 (2001) doi: https://doi.org/10.1103/PhysRevB.65.012301
29. V. Schott, M. Fähnle, P.A. Madden, J. Phys. Condens. Matter **12**, 1171 (2000). https://doi.org/10.1088/0953-8984/12/7/303
30. G. Göltz, A. Heidemann, H. Mehrer, A. Seeger, D. Wolf, Philos. Mag. A **41**, 723 (1980). https://doi.org/10.1080/01418618008239345